

Three-Dimensional Monte Carlo Simulation of Submicronic Devices

C. Brisset, P. Dollfus, N. Chemarin, R. Castagné, and P. Hesto

Institut d'Electronique Fondamentale, CNRS URA022, Université Paris-Sud
Bât 220, F-91405 Orsay Cédex, FRANCE

Abstract

Our particle Monte-Carlo program for device modelling (MONACO) has been extended to the third dimension in geometric space. We describe the main features of this model. It has been used to simulate a $0.1\ \mu\text{m}$ -gate-width N-channel MOSFET. Important geometric edge effects occur and induce a reduction of the effective gate width.

1. Introduction

The scaling down in present ULSI technologies' constrains the device physicists to take into account at the same time the non-stationary transport ^{/1-3/} and the three-dimensional effects in the geometric space ^{/4,5/}. The particle ensemble Monte-Carlo technique is actually the most accurate device modeling method that can meet these requirements. So, we have extended our particle Monte-Carlo model to three-dimensional (3D) simulations. Some important points of this new 3D model are presented. We described also some precautions that must be taken to obtain accurate simulation results. Finally, we present a steady-state analysis of a N-channel MOSFET having a short gate width ($W=0.1\ \mu\text{m}$) and a small ratio W/L ($W/L=0.1$). This analysis shows off important edge effects that influence the device performances.

2. The model

The carrier motion, that was previously described ^{/2,6/}, is unchanged. The potential distribution in the device is calculated from Poisson's equation using a finite-element formulation in a non-uniform rectangular meshing. Poisson's equation is then solved using a L.U. method. The electric field components are calculated by derivation of the distribution potential. A rectangular meshing facilitates the detection of the cell changes during the motion of each carrier, which is required to up-date the local electric field acting on the carrier. The boundary conditions in the solution of Poisson's equation consist in imposing the potential at every contact surface (Dirichlet condition). Elsewhere on the boundary the normal component of the electric field is taken equal to zero (Neumann condition). Consistently with Neumann condition a carrier reaching such a boundary is reflected. A carrier reaching an ohmic contact is free to leave the device through this

contact. In the cells adjacent to an ohmic contact the equilibrium carrier concentration is assumed to be recovered ($n=N_D$ or $p=N_A$). So, before each resolution of Poisson's equation, a lack of carriers appearing in such a cell is compensated by injection of carriers. Its initial energy and momentum are specified by a Maxwellian distribution. This last boundary condition is the only condition of injection of carriers in the device.

As in all dynamic model based on the solution of Poisson's equation the time and spatial grids must meet requirements related to physical constants of time and spatial relaxation. In one hand, the time step Δt between two up-dates of the electric field distribution must not be greater than the dielectric relaxation time in the heavily doped regions ($\Delta t \approx 5$ fs for a doping level of 10^{18} cm $^{-3}$ in Si). This ensures that the carrier population can relax after every local perturbation without error due to the "frozen" local field. In the other hand, in regions where the potential is likely to vary spatially, the mesh size must be less than the length of variation, i.e., the Debye length (L_D) that can be as small as 4 nm for a carrier concentration of 10^{18} cm $^{-3}$.

Furthermore the choice of the volume of the cells adjacent to ohmic contacts appears (especially in 3D modelling). It is related to the particle nature of the model and to the boundary conditions applied at ohmic contacts. As above mentioned, a lack of carrier in a cell adjacent to an ohmic contact is quasi-immediately compensated by injection of carrier. Such an algorithm leads to an average excess of about one carrier compared to the equilibrium number n_0 (that corresponds to a number of particle n equal to the number of impurities N_D). The system tends to relax the relative excess of carrier equal to $1/n_0$ by re-adjustment of the electric field. This effect is of course all the more important that n_0 is low.

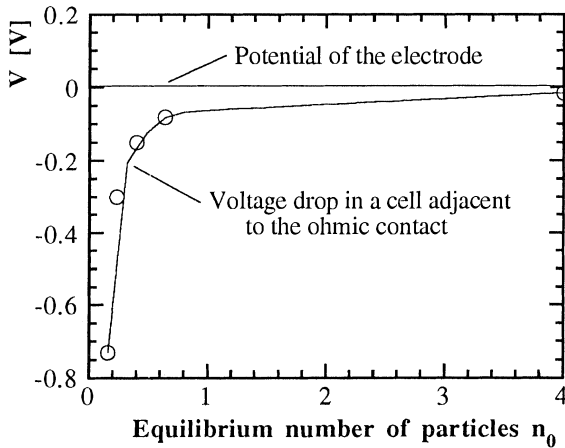


Figure 1: Voltage drop in a cell adjacent to an ohmic contact ($N_D=10^{18}$ cm $^{-3}$) as a function of the equilibrium number of particles n_0 .

In Fig.1 the voltage drop in a cell adjacent to an ohmic contact ($N_D=10^{18}$ cm $^{-3}$) is plotted as a function of the equilibrium number of particles n_0 . The variation of n_0 was obtained by varying the mesh spacing. For $n_0 \leq 1$ the voltage drop increases rapidly with decreasing n_0 , which can lead to strong perturbations in the overall potential and carrier distribution in the device. A value of n_0 greater than one seems to be required to maintain low levels of potential fluctuations in ohmic contacts.

The choice of the cell sizes L is thus subject to two conditions: (i): $L \leq L_D$ in regions where the potential is likely to vary. (ii) the cell volume must be large enough near ohmic contacts so that $n_0 > 1$.

3. 3D modeling of a N-MOSFET

To point out the three-dimensional effects, we have compared the behavior of two N-channel MOSFETs using the 3D algorithm. The gate length and the oxide thickness are respectively $1 \mu\text{m}$ and 20 nm . The doping level of acceptor impurities in the channel is $N_A = 4 \times 10^{16} \text{ cm}^{-3}$. The N^+ regions of source and drain contacts are doped to $N_D = 10^{18} \text{ cm}^{-3}$. The gate width of the first MOSFET is assumed to be boundless. In fact we have simulated only a $0.3 \mu\text{m}$ wide slice with imposing Neumann boundary conditions at the edge of the device perpendicular to the gate length. The gate width of the second MOSFET is limited to $0.1 \mu\text{m}$ ($W/L=0.1$) all other things being equal. The drain characteristics in both cases well saturate. The transfer characteristics of both transistors are plotted in Fig.2. For comparison, the currents are plotted for a normalized gate width of 1 mm . One can notice that the drain currents are smaller for the $0.1 \mu\text{m}$ -gate-width MOSFET (at least 30% smaller according to V_{GS}). The lower currents are due to a reduction of the effective gate width, which is shown in Fig.3. It is a plot of the potential and electron concentration in the inversion layer along the width of the device ($V_{GS} = V_{DS} = 5 \text{ V}$). The voltage drop between the gated and the ungated region is partially applied on the gate edges, which originates the reduction of the effective gate width. This effect induces also a shift of threshold voltage. The values of V_T can be derived from the square of the drain current against V_{GS} curves. The $0.1 \mu\text{m}$ -gate-width device exhibits a value of V_T greater than the boundless gate device of about 0.3 V (1.3 V instead of 1 V).

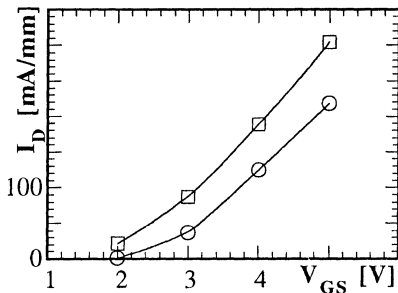


Figure 2: Transfer characteristics of the boundless gate width MOSFET (squares) and the $0.1 \mu\text{m}$ gate width MOSFET (circles).

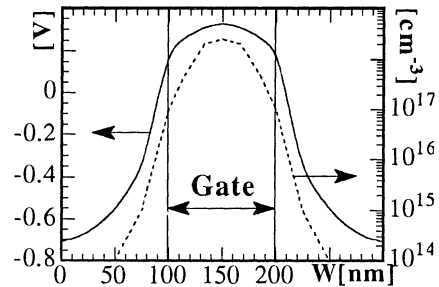


Figure 3: Potential (solid line) and electron concentration (dashed line) in the inversion layer along the width in the middle of the device.

Another 3D effect occurs beyond the pinch-off point at the end of the channel near the drain of the $0.1 \mu\text{m}$ gate width MOSFET; the current partially flows down into the bulk of the device (Fig.4a), as in large gate width MOSFET, but also spreads outside the gate (Fig.4b).

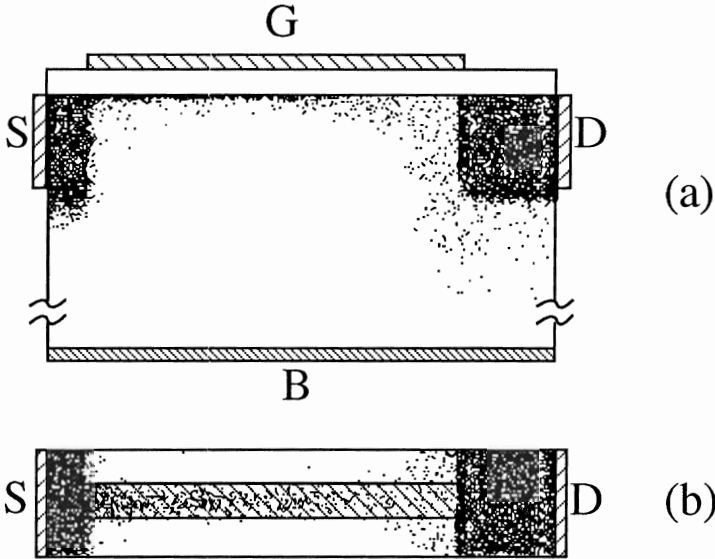


Figure 4: The electron distribution in the $0.1 \mu\text{m}$ gate width MOSFET for $V_{GS}=5 \text{ V}$ and $V_{DS}=5 \text{ V}$.

4. Conclusion and perspectives

Despite its large computational requirements, the 3D particle Monte-Carlo model is very suitable for studies of actual and future low size devices that can be subject to important 3D effects and non-stationary transport effects. We have presented the case of a small gate width MOSFET that could be designed for integrated circuits. This model could also treat effectively the case of nanometric gate FETs intended for microwave applications, for which $W/L \gg 1$ is required. In such conditions the fluctuations of gate length along the width could perturb the device operating and performances. Our model is also suitable to the analyze of the behavior of devices under radiation that is a 3D phenomena.

References

- [1] P.Dollfus, C.Bru, and P.Hesto, *J.Appl.Phys.*, vol.73,p.804, 1993
- [2] L.Rajaonarison, P.Hesto, J.F.Pône, and P.Dollfus, *SISDEP 91*, vol.4, p.513, 1991
- [3] H.Sheng, R.Guerrieri, and A.Sangiovanni-Vincentelli *SISDEP 91*, vol.4, p.285, 1991
- [4] H.C.Chan, and T.J.Shieh, *IEEE Trans. Electron Devices*, vol.38,p.2427, 1993
- [5] H.Matsuo, J.Tanaka, A.Mishima, K.Tago, and T.Toyabe *SISDEP 91*, vol.4, p.165, 1991
- [6] P.Hesto, J.F.Pône, M.Mouis, J.L.Pelouard, and R.Castagné, *NASECODE IV*, (Boole Press, Dublin, 1985), p.315, 1985